PHYSICAL REVIEW D **84,** 033012 (2011)

Neutrino production of single pions: Dipole description

B. Z. Kopeliovich,* Ivan Schmidt,† and M. Siddikov‡

Departamento de Física, Instituto de Estudios Avanzados en Ciencias e Ingeniería, y Centro Científico - Tecnológico de Valparaíso, Universidad Técnica Federico Santa María, Casilla 110-V, Valparaíso, Chile

(Received 18 July 2011; published 22 August 2011)

The light-cone distribution amplitudes for the axial current are derived within the instanton vacuum model, which incorporates nonperturbative effects including spontaneous chiral symmetry breaking. This allows one to extend applicability of the dipole approach, usually used in the perturbative domain, down to $Q^2 \to 0$, where the partially conserved axial current imposes a relation between the neutrino-production cross section and the one induced by pions. A dramatic breakdown of the Adler relation for diffractive neutrino production of pions, caused by absorptive corrections, was revealed recently by Kopeliovich *et al.*. Indeed, comparing with the cross section predicted by the dipole phenomenology at $Q^2 \to 0$ on a proton target we confirmed the sizable deviation from the value given by the Adler relation, as was estimated by Kopeliovich *et al.* within a simplified two-channel model. The dipole approach also confirms that in the black-disk limit, where the absorptive corrections maximize, the diffractive cross section ceases, on the contrary to the expectation based on the partially conserved axial current.

DOI: 10.1103/PhysRevD.84.033012 PACS numbers: 13.15.+g, 13.85.−t

I. INTRODUCTION

Because of its V-A shape the neutrino-hadron interactions possess a very rich structure. However, because of the smallness of the cross sections until recently the experimental data have been scarce, mostly being limited to the total cross sections. With the launch of the new high-statistics experiments such as MINERvA at Fermilab [1], now the neutrino-hadron interactions may be studied with a better precision. The V-A structure of the neutrino-quark vertices enables us to study simultaneously $\langle VV\rangle$, $\langle AA\rangle$, and $\langle VA\rangle$ correlators in the same process.

The properties of the vector current have been well studied in the processes of deep inelastic scattering (DIS) of leptons on protons and nuclei, deeply virtual Compton scattering, real Compton scattering, and vector meson production. The standard approach in the description of such processes is based on the large-Q^2 factorization of the cross section into a process-dependent hard part, which is evaluated in perturbative QCD (pQCD), and a universal target-dependent soft part. The latter is extracted from fits to experimental data. Factorization, however, is not valid at small photon virtualities, where one can rely on the dispersion relation, or on the assumption of generalized vector meson dominance (GVMD) [2–5]. Such a description, however, involves a lot of *ad hoc* modeling.

An alternative phenomenology for high-energy QCD processes is based on the color dipole approach [6]. One assumes that before interaction, the projectile (virtual W or Z boson in the case of the neutrino scattering) fluctuates into a quark-antiquark dipole. After the dipole is formed, it scatters in the field of the target and then fluctuates back to the final hadron [6]. Recently the color dipole approach has been successfully applied to the description of different reactions with vector currents (see [7–26] and references therein).

For the axial current the situation is more complicated, especially at small Q^2, because the chiral symmetry breaking generates the near-massless pseudogoldstone mesons (pions). Straightforward extension of the vector dominance model to the axial current leads to the so-called Piketty-Stodolsky paradox [27,28]that appears because axial meson dominance is broken by a large contribution of multipion singularities in the dispersion relation [28,29]. The dipole description is free of this problem, because in this model there is no explicit hadronic degrees of freedom and the interaction occurs via dipole scattering.

According to the Adler theorem [30,31], based on the hypothesis of partial conservation of the axial current (PCAC), the neutrino-proton interactions cross section at zero Q^2 is proportional to the cross section of the pure hadronic process, where the heavy intermediate boson is replaced by a pion,

$$\nu\frac{d\sigma_{\nu p\to lF}}{d\nu dQ^2}\bigg|_{Q^2=0}=\frac{G_F^2}{2\pi^2}f_\pi^2(1-y)\sigma_{\pi p\to F}(\nu), \qquad (1)$$

where F denotes the final hadronic state, $y=\nu/E_\nu$, E_ν is the energy of the neutrino, and ν is the energy of the heavy boson W, or Z, in the target rest frame. The chiral symmetry is vital and should be embedded into any dynamical model which is used for calculation of the cross section at small Q^2.

In what follows we entirely neglect the lepton mass (accurate for neutral currents or electrons), which can be easily incorporated [27], but is dropped for the sake of simplicity. If one interpreted the Adler relation (AR)

*Boris.Kopeliovich@usm.cl
†Ivan.Schmidt@usm.cl
‡Marat.Siddikov@usm.cl

[Eq. (1)] in terms of pion pole dominance, one would arrive at a vanishing cross section. Indeed, the pion pole term in the amplitude contains a factor q_μ, which multiplied by the conserved lepton current l_μ terminates this contribution [27,28,32,33]. Other, heavier meson states provide a final contribution, but have to conspire to mimic the pion pole term, as dictated by the PCAC relation Eq. (1).

Such a fine-tuning looks miraculous if one has no clue of the underlying dynamics. A similar paradox is known for the $1/Q^2$ behavior of the DIS cross section. In QCD this is known as a result of color screening [6], leading to the effect called color transparency. While this is rather obvious within the color dipole description, it becomes extremely sophisticated in hadronic representation. Indeed, expanding the current over hadronic states one may arrive at a problem called Bjorken paradox [34]. Namely, how it happens that many hadronic states, having large sizes and large cross sections, conspire in a way that all together they act like a small hadron with a tiny, $\sim 1/Q^2$ cross section. The solution is known, the off-diagonal diffractive amplitudes are negative and cancel with diagonal ones [35]. This however cannot be proven, unless one employs an explicit model describing the features of the hadronic states and the diffractive amplitudes. This is why the color transparency effect has not been understood within the GVMD, but was revealed in the color dipole representation [6].

Similarly, in order to test the mysterious relation between the contribution of heavy hadronic fluctuations and pion, one should switch to the dipole representation and employ models for the distribution amplitudes (DA) of the axial current which have built-in chiral symmetry. Recently, we used the DA of the vector current calculated in the instanton vacuum model (IVM) for the evaluation of several processes [10–13]. In this paper we apply the IVM to construct the DAs for the axial current and pion and use them to calculate the neutrino-production cross sections. Since the IVM includes spontaneous chiral symmetry breaking, the $\bar{q}q$ DAs of axial current and pion should automatically satisfy the PCAC, and in the small-Q^2 limit reproduce the Adler relation (1).

Notice that the color dipole description is valid only at high energies or at small $x_B \ll 1$, where the contribution of quark exchange (Reggeons) is suppressed as $1/\sqrt{\nu}$. For moderate energies other mechanisms, such as e.g. formation of resonances in the direct channel, and/or Reggeon exchange in the crossed channel may be important. In this paper we do not consider those corrections, but concentrate on the well-developed small-x dipole phenomenology.

Experimentally, the neutrino production of hadrons on protons and nuclei has been studied in the recent experiments K2K [36–38], MiniBoone [39,40], and NuTeV [41–43] (see also the review [28] and [29,44–47] for references to earlier neutrino experiments). For high-energy neutrino scattering, there are data from the early bubble chamber experiments [33,48] with energies up to 100 GeV, though with low statistics and only for the total (integrated) cross sections. Currently, with the launch of the high-statistics experiment Minerva at Fermilab [1,26], the precision of measurements should be considerably improved, and data for the differential cross sections at high energies will become available.

In this paper we consider a particular process—the diffractive single pion production on a proton target. As was demonstrated by Kopeliovich *et al.*[32], this process provides a most sensitive way to test PCAC in high-energy neutrino interactions. Besides, it generates an important background to the measurements of neutrino oscillations [49–52], and is also important for the neutrino astronomy of astrophysical and cosmological sources.

This paper is organized as follows. In Sec. II we present the color dipole formalism. In Sec. III we perform calculations of the DAs of the axial current and pion. In Sec. IV we calculate the overlap of the DAs for the axial current and the pion and found it to be proportional to q_μ, what terminates this contribution to the neutrino production of pions due to conservation of lepton current. In Sec. V we present the numerical results and summarize the observations in Sec. VI.

II. DIFFRACTIVE PRODUCTION OF PIONS

The cross section of diffractive neutrino production of a pion on a proton, $\nu p \to l\pi p$, has the form,

$$\nu \frac{d^3\sigma_{\nu p\to\mu\pi p}}{d\nu dt dQ^2} = \frac{G_F^2 L_{\mu\nu}(W_\mu^A)^* W_\nu^A}{32\pi^3 m_N^2 E_\nu^2 \sqrt{1+Q^2/\nu^2}}, \qquad (2)$$

where m_N is the nucleon mass, $L_{\mu\nu}$ is the lepton tensor, and W_μ^A is the amplitude of pion production by the axial current on the proton target. In the color dipole model this amplitude has the form

$$W_\mu^A(s,\Delta,Q^2) = \int_0^1 d\beta_1 d\beta_2 d^2r_1 d^2r_2 \bar{\Psi}^\pi(\beta_2,\vec{r}_2) \times \mathcal{A}^d(\beta_1,\vec{r}_1;\beta_2,\vec{r}_2;\Delta)\Psi_\mu^A(\beta_1,\vec{r}_1), \qquad (3)$$

where $\bar{\Psi}^\pi$ and Ψ_μ^A are the DAs of the pion and axial current, respectively, and $\mathcal{A}^d(\cdots)$ is the dipole scattering amplitude. The axial current DA Ψ_μ^A contains a pion pole, whose contribution to the amplitude is proportional to q_μ, because the pion is spinless. This factor terminates the pion pole because of conservation of the lepton current. As we assumed, the lepton is massless; otherwise the pion pole contribution is not zero and leads to corrections of the order of $\mathcal{O}[m_l^2/(m_\pi^2+Q^2)]$ [27].

The amplitude $\mathcal{A}^d(\beta_1,\vec{r}_1;\beta_2,\vec{r}_2;\Delta)$ in (3) depends on the initial and final quark transverse separations $\vec{r}_{1,2}$, fractional light-cone momenta $\beta_{1,2}$, and transverse momentum transfer $\vec{\Delta}$. This is a universal function dependent only on the target but not on the initial and final states. In addition to the axial current contribution, in (3) there should be the

contribution of the vector current. This contribution involves a poorly known helicity flip dipole amplitude $\tilde{\mathcal{A}}_d$, which vanishes at high energies as $1/\nu$. Besides, at small Q^2, the vector current contribution is suppressed by a factor Q^2. At high energies, in the small angle approximation, $\Delta/\sqrt{s} \ll 1$, and the quark separation and fractional momenta β are preserved, so

$$\mathcal{A}^d(\beta_1, \vec{r}_1; \beta_2, \vec{r}_2; Q^2, x, \Delta) \approx \delta(\beta_1 - \beta_2)\delta(\vec{r}_1 - \vec{r}_2)(\epsilon + i)\mathrm{Im}f^N_{\bar{q}q}(\vec{r}, \vec{\Delta}, \beta, x), \quad (4)$$

where ϵ is the ratio of the real to imaginary parts, and for the imaginary part of the elastic dipole amplitude we employ the model developed in [10,53–55],

$$\mathrm{Im}f^N_{\bar{q}q}(\vec{r}, \vec{\Delta}, \beta, x) = \frac{\sigma_0(x)}{4}\exp\left[-\left(\frac{B(x)}{2} + \frac{R_0^2(x)}{16}\right)\vec{\Delta}_\perp^2\right] \times (e^{-i\beta\vec{r}\cdot\vec{\Delta}} + e^{i(1-\beta)\vec{r}\cdot\vec{\Delta}} - 2e^{i(1/2)-\beta\vec{r}\cdot\vec{\Delta}}e^{-r^2/R_0^2(x)}). \quad (5)$$

The phenomenological functions $\sigma_0(x)$, $R_0^2(x)$, and $B(x)$ are fitted to DIS and ρ electroproduction data. We rely here on the Bjorken variable $x = Q^2/2(pq)$, which has the meaning of fractional light-cone momentum of the parton only at large Q^2. At low Q^2 important for the axial current, one should switch to an energy dependent parametrization, as explained in Sec. V.

For the forward scattering, $\Delta \to 0$, the imaginary part of the amplitude (4) reduces to the saturated pparametrization of the dipole cross section proposed by Golec-Biernat and Wüsthoff (GBW) [7],

$$\sigma_d(r, x) = \mathrm{Im}f^N_{\bar{q}q}(\vec{r}, \vec{\Delta} = 0, \beta, x) = \sigma_0(x)\left[1 - \exp\left(-\frac{r^2}{R_0^2(x)}\right)\right]. \quad (6)$$

Generally speaking, the amplitude $f^N_{\bar{q}q}(\cdots)$ involves nonperturbative physics, but its asymptotic behavior at small r is controlled by pQCD [6]:

$$f^N_{\bar{q}q}(r)_{r\to 0} \propto r^2,$$

up to slowly varying factors $\sim \ln(r)$ [6].

Calculation of the differential cross section also involves the real part of the scattering amplitude, whose relation to the imaginary part is quite straightforward. According to [56], if $\lim_{s\to\infty}(\mathrm{Im}f/s^\alpha)$ is finite, then the real and imaginary parts of the forward amplitude are related as

$$\mathrm{Re}\, f(\Delta = 0) = s^\alpha \tan\left[\frac{\pi}{2}\left(\alpha - 1 + \frac{\partial}{\partial \ln s}\right)\right]\frac{\mathrm{Im}f(\Delta = 0)}{s^\alpha}. \quad (7)$$

In the model under consideration the imaginary part of the forward dipole amplitude indeed has a power dependence on energy, $\mathrm{Im}f(\Delta = 0; s) \sim s^{\alpha_{\mathbb{P}}-1}$, where $\alpha_{\mathbb{P}}$ is the intercept of the effective Pomeron trajectory. Then Eq. (7) simplifies to

$$\frac{\mathrm{Re}\mathcal{A}}{\mathrm{Im}\mathcal{A}} = \tan\left(\frac{\pi}{2}(\alpha_{\mathbb{P}} - 1)\right) \equiv \epsilon. \quad (8)$$

This fixes the phase of the forward scattering amplitude, which we retain for nonzero momentum transfer, assuming similar Δ dependences for the real and imaginary parts.

III. DISTRIBUTION AMPLITUDES AND THE INSTANTON VACUUM MODEL

In this section we define the DAs and give a brief description of the instanton model used for their evaluation (see [57–59] and references therein).

A. Instanton vacuum model

The central object of the model is the effective action for light quarks in the instanton vacuum, which in the leading order in N_c has the form [58,59]

$$S = \int d^4x\left(\frac{N}{V}\ln\lambda + 2\Phi^2(x) - \bar{\psi}(\hat{p} + \hat{v} + \hat{a}\gamma_5 - m - c\bar{L}f \otimes \Phi\cdot\Gamma_m \otimes fL)\psi\right), \quad (9)$$

where Γ_m is one of the matrices, $\Gamma_m = 1, i\vec{\tau}, \gamma_5, i\vec{\tau}\gamma_5$; ψ and Φ are the fields of constituent quarks and mesons, respectively; N/V is the density of the instanton gas; $m \approx 5$ MeV is the current quark mass; and $\hat{v} \equiv v_\mu\gamma^\mu$ is the external vector current corresponding to the photon. L is the gauge factor defined as

$$L(x, z) = P\exp\left(i\int_z^x d\zeta^\mu(v_\mu(\zeta) + a_\mu(\zeta)\gamma_5)\right), \quad (10)$$

$$\bar{L}(x, z) = \gamma_0 L^\dagger(x, z)\gamma_0. \quad (11)$$

It provides the gauge invariance of the action, and $f(p)$ is the Fourier transform of the zero-mode profile in the single-instanton background. In this paper we used for evaluations the dipole-type parametrization [58]

$$f(p) = \frac{L^2}{L^2 - p^2}$$

with $L \sim 850$ MeV.

In the leading order in N_c, we have the same Feynman rules as in the perturbative theory, but with a momentum-dependent quark mass $\mu(p)$ in the quark propagator

$$S(p) = \frac{1}{\hat{p} - \mu(p) + i0}. \quad (12)$$

The mass of the constituent quark has the form

$$\mu(p) = m + Mf^2(p),$$

where $m \approx 5$ MeV is the current quark mass, and $M \approx 350$ MeV is the dynamical mass generated by the interaction with the instanton vacuum background. Because of the presence of the instantons the vector current–quark coupling is also modified,

$$\hat{v} \equiv v_\mu \gamma^\mu \to \hat{V} = \hat{v} + \hat{V}^{\rm nonl},$$
$$\hat{a} \equiv a_\mu \gamma^\mu \to \hat{A} = \hat{a} + \hat{A}^{\rm nonl}.$$

In addition to the vertices of the perturbative QCD, the model contains the nonlocal terms with higher-order couplings of currents to mesons. The exact expressions for the nonlocal terms $\hat{V}^{\rm nonl}$, $\hat{A}^{\rm nonl}$ depend on the choice of the path in (10), so one can find different results in the literature [60–63]. However, for the longitudinal parts of the axial and vector currents important here, this ambiguity cancels out and couplings have the form

$$\hat{V}_{\rm nonl} = v_\mu \left[iM \frac{p_1^\mu + p_2^\mu}{p_2^2 - p_1^2} (f(p_2)^2 - f(p_1)^2) \right],$$
$$\hat{A}_{\rm nonl} = a_\mu \left[iM \frac{p_1^\mu + p_2^\mu}{p_2^2 - p_1^2} (f(p_2) - f(p_1))^2 \right],$$

where p_1, p_2 are the momenta of the initial and final quarks.

B. Axial current distribution amplitudes

The distribution amplitudes of the axial current are defined via 3-point correlators

$$\Psi_\beta \sim \int d^4\xi e^{-iq\cdot\xi} \langle 0|\bar{\psi}(y)\Gamma\psi(x) J^5_\beta(\xi)|0\rangle, \tag{13}$$

where $J^5_\beta(\xi)$ is the axial isovector current and Γ is one of the Dirac matrices. Because of the spontaneous chiral symmetry breaking and existence of the near-massless pions the hadronic structure of the axial current differs from that of the vector current. In particular, the axial current may fluctuate into the pion state before production of the $\bar{q}q$ pair. Thus the correlator (13) has two contributions, schematically shown in Fig. 1.

One term corresponds to the combined contribution of the intermediate heavy states (a_1 meson, 3π, etc.), and another one corresponds to the axial current fluctuating into a pion. Because of the built-in chiral symmetry, the two contributions are connected by PCAC, so for the full DA we have

$$\Psi_\mu = \Psi_\mu^{\rm (bulk)} + \Psi_\mu^{\rm (pion)} = \left(g_{\mu\nu} - \frac{q_\mu q_\nu}{q^2 - m_\pi^2} \right) \Psi_\nu^{\rm (bulk)}. \tag{14}$$

This form of the DA reflects the relation between the pion pole and the bulk of heavy states contribution imposed by PCAC, which has been discussed above. In what follows we concentrate on the part of the amplitude presented in the dispersion relation by the bulk of heavy states excluding the pion pole (left panel of Fig. 1), tacitly assuming that the full distribution amplitudes are determined using (14).

For the part of the axial current presented by the bulk of heavy states, the DAs may be defined similar to the distribution amplitudes of the axial meson [64]:

$$\langle 0|\bar{\psi}(y)\gamma_\mu\gamma_5\psi(x)|A(q)\rangle = if_A^2 \int_0^1 d\beta e^{i(\beta p\cdot y + \bar{\beta} p\cdot x)} \left[p_\mu \frac{e^{(\lambda)}\cdot z}{p\cdot z} \Phi_{||}(\beta) + e_\mu^{(\lambda=\perp)} g_\perp^{(a)}(\beta) - \frac{1}{2} z_\mu \frac{e^{(\lambda)}\cdot z}{(p\cdot z)^2} f_A^2 g_3(\beta) \right], \tag{15}$$

$$\langle 0|\bar{\psi}(y)\gamma_\mu\psi(x)|A(q)\rangle = -if_A^2 \epsilon_{\mu\nu\rho\sigma} e_\nu^{(\lambda)} p_\rho z_\sigma \int_0^1 d\beta e^{i(\beta p\cdot y + \bar{\beta} p\cdot x)} \frac{g_\perp^{(v)}(\beta)}{4}, \tag{16}$$

$$\langle 0|\bar{\psi}(y)\sigma_{\mu\nu}\gamma_5\psi(x)|A(q)\rangle = f_A \int_0^1 d\beta e^{i(\beta p\cdot y + \bar{\beta} p\cdot x)} \left[(e_\mu^{(\lambda=\perp)} p_\nu - e_\nu^{(\lambda=\perp)} p_\mu) \Phi_\perp(\beta) + \frac{e^{(\lambda)}\cdot z}{(p\cdot z)^2} f_A^2 (p_\mu z_\nu - p_\nu z_\mu) h_{||}^{(t)}(\beta) + \frac{1}{2} (e_\mu^{(\lambda)} z_\nu - e_\nu^{(\lambda)} z_\mu) \frac{f_A^2}{p\cdot z} h_3(\beta) \right], \tag{17}$$

$$\langle 0|\bar{\psi}(y)\gamma_5\psi(x)|A(q)\rangle = f_A^3 e^{(\lambda)}\cdot z \int_0^1 d\beta e^{i(\beta p\cdot y + \bar{\beta} p\cdot x)} \frac{h_{||}^{(p)}(\beta)}{2}, \tag{18}$$

where q is the momentum carried by the axial current; β is the fractional light-cone momentum; $\bar{\beta} \equiv 1 - \beta$, $e^{(\lambda)} \equiv e^{(\lambda)}(q)$ is the polarization vector of the axial meson with polarization state λ; $z = x - y$; p_μ is the "positive" direction vector on the light cone; and n_μ is the "negative" direction vector on the light cone. Light cone vectors p and n are chosen in such a way that the vector q does not have transverse components. The normalization constant f_A is a dimensional parameter introduced in order to make the distribution amplitudes dimensionless. Its value is fixed from the condition

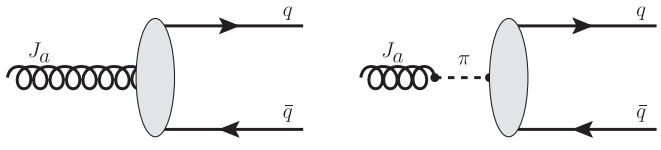

FIG. 1. The distribution amplitude has two contributions, with intermediate heavy axial states and with a pion, referred to in the text as (bulk) and (pion), respectively.

$$\int_0^1 d\beta \Phi_{\|}(\beta) = 1. \tag{19}$$

We defined an "effective" axial state $|A^{(\lambda)}(q)\rangle$ as

$$|A^{(\lambda)}(q)\rangle = \int d^4x e^{-iq\cdot x} e_\beta^{(\lambda)}(q) J_\beta^5(x)|0\rangle. \tag{20}$$

The DAs have the following twists: $\Phi_{\|}(\beta)$, $\Phi_\perp(\beta)$ are twist-2; $g_\perp^{(a)}$, $g_\perp^{(v)}$, $h_{\|}^{(t)}$, and $h_{\|}^{(p)}$ are of twist-3; and g_3, h_3 are of twist-4. All the wave functions in (15) and (16) are chiral even; all the wave functions in (17) and (18) are chiral odd.

C. Pion distribution amplitudes

A spinless pion has only four independent DAs defined as [65]

$$\langle 0|\bar\psi(y)\gamma_\mu\gamma_5\psi(x)|\pi(q)\rangle = if_\pi \int_0^1 d\beta e^{i(\beta p\cdot y+\bar\beta p\cdot x)}\left(p_\mu \phi_{2;\pi}(\beta) + \frac{1}{2}\frac{z_\mu}{(p\cdot z)}\psi_{4;\pi}(\beta)\right), \tag{21}$$

$$\langle 0|\bar\psi(y)\gamma_5\psi(x)|\pi(q)\rangle = -if_\pi \frac{m_\pi^2}{m_u+m_d}\int_0^1 d\beta e^{i(\beta p\cdot y+\bar\beta p\cdot x)}\phi_{3;\pi}^{(p)}(\beta), \tag{22}$$

$$\langle 0|\bar\psi(y)\sigma_{\mu\nu}\gamma_5\psi(x)|\pi(q)\rangle = -\frac{i}{3}f_\pi \frac{m_\pi^2}{m_u+m_d}\int_0^1 d\beta \phi_{3;\pi}^{(\sigma)}(\beta)\frac{e^{i(\beta p\cdot y+\bar\beta p\cdot x)}}{p\cdot z} \times (p_\mu z_\nu - p_\nu z_\mu). \tag{23}$$

Twist counting is the following: $\phi_{2;\pi}$ is a single twist-2 function (it was evaluated earlier in [66–68]), $\phi_{3;\pi}^{(p)}$ and $\phi_{3;\pi}^{(\sigma)}$ are twist-3, and $\psi_{4;\pi}$ is the twist-4 DA.

The full expressions for the DAs (15), (17), (16), (18), and (21)–(23) are given in Secs. A 1 and A 2 of the Appendix.

The DAs for the vector current are presented in Sec. A 3 of the Appendix. However, the vector current does not contribute to the color dipole amplitudes of pion production. Although it contains nonzero components, their overlap with the pion DAs is zero. The vector part vanishes because the color dipole amplitude does not flip helicity. Within the vector dominance model approximation such components may be expressed via the $\rho N \to \pi N$ scattering amplitudes, which exist only due to quark-antiquark (Reggeon) exchange in the cross channel. This is beyond the employed dipole phenomenology corresponding to gluonic (Pomeron) exchanges.

IV. DISAPPEARANCE OF THE PION POLE IN THE DIPOLE REPRESENTATION

As emphasized above, the pion pole contribution to the pion production amplitude vanishes because of lepton current conservation (up to the lepton mass). This nontrivial observation of [27,28,32,33] is in variance with the naive interpretation of the AR Eq. (1), which relates diffractive neutrino production of pions, $\nu + p \to l + \pi + p$, with elastic pion-proton scattering, $\pi + p \to \pi + p$. It is tempting to interpret this relation as pion pole dominance, i.e. the neutrino fluctuates to a pion, which then interacts elastically with the proton target. If this were true, the amplitude should be maximized in the so-called black disk limit, which corresponds to unitarity saturation when the imaginary part of the partial elastic amplitude reaches the maximal value allowed by the unitarity relation.

On the other hand, if the pion pole does not contribute [27,28,32,33] as is stressed above, all hadronic fluctuations of the neutrino contributing to $\Psi^{(\mathrm{bulk})}$ are heavier than a pion, so all diffractive hadronic amplitudes of pion production are off diagonal. Such amplitudes vanish in the black-disk limit, so the pion cannot be produced diffractively. The source of such a dramatic breakdown of PCAC was identified in [32] as a result of strong absorptive corrections. Of course the deviation from the PCAC prediction, AR, on a proton or nuclear targets, which may be far from the unitarity bound, is not so dramatic, as was calculated in [32].

In this section we present an explicit demonstration of disappearance of diffractive pion production in the black-disk limit relying on the dipole model. Namely, in this regime all the partial elastic amplitudes (5) reach the unitarity bound, becoming independent of the dipole transverse separation $\vec r$, and Eq. (3) simplifies to just an overlap of the initial (axial current) and final (pion) light-cone wave function. We intent to demonstrate that this overlap vanishes.

The amplitude of pion production in this regime has the form,

$$F_\mu^{J_A\to\pi}(q,\Delta) = \sum_a \int d\beta d^2r \bar\Psi_\pi^{(a)}(\beta,\vec r; q-\Delta)\Psi_{\mu,A}^{(a)}(\beta,\vec r; q), \tag{24}$$

where the index a numerates all the distribution amplitudes. This is suppressed, since transition from spin-1 to spin-0 requires helicity flip for one of the quarks in the quark-antiquark pair. Now we demonstrate explicitly that such suppression indeed takes place in the case of the perturbative QCD model.

The distribution amplitude of the meson state is defined as

$$\int dz e^{i\beta z} e^{i\vec k\vec r}\langle 0|\bar\psi(z,\vec r)\Gamma\psi(0)|M(q)\rangle = \Phi_M(\beta,\vec r; q), \tag{25}$$

FIG. 2. Diagram corresponding to the distribution amplitude (25) in pQCD.

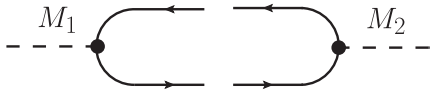

FIG. 3. Diagram corresponding to the overlap of the distribution amplitudes.

where the separation between the quark and antiquark has a ''minus'' and transverse components (z, r), and Γ is one of the Dirac matrices $(1, \gamma^5, \gamma_\mu, \gamma_\mu\gamma_5, \sigma_{\mu\nu})$ multiplied by the proper isospin factor (for the isoscalar this is 1, for isovector mesons it is $i\vec{\tau}$, etc.). The exact expression on the right-hand side depends on the matrix Γ, the spin of the meson, and is usually given as a twist expansion over all possible Lorentz structures which may be constructed from Γ, q, $\vec{r}$ and the polarization vector $\epsilon(q)$.

In the leading order of α_s (which is justified for very large q^2) the corresponding DA may be represented as a simple diagram shown schematically in Fig. 2. Then we have

$$\Phi_M(\beta, \vec{r}; q) \sim \int d^4k\delta(\beta - k^+/q^+)e^{ik_\perp r_\perp}\,\mathrm{Tr}[S(k)\Gamma_M S(k-q)\Gamma]$$
$$= \int d^2k_\perp e^{ik_\perp r_\perp}\int dk^- \frac{f(k,q)}{(2k^+k^- - k_\perp^2 - m^2 + i0)(2(k^+ - q^+)(k^- - q^-) - (k_\perp + q_\perp)^2 - m^2 + i0)}, \quad (26)$$

where the function $f(k, q) = \langle(\hat{k} + m)\Gamma(\hat{k} + \hat{q} + m)\Gamma_M\rangle$ depends on the spins of mesons and Dirac matrices and is not important for a moment.

Taking the integral over k^-, we get

$$\int d^4k\delta(\beta - k^+/q^+)e^{ik_\perp r_\perp}\,\mathrm{Tr}[S(k)\Gamma_M S(k-q)\Gamma] = \theta(0 \le \beta \le 1)\int d^2k_\perp e^{ik_\perp r_\perp}\frac{f(k,q)}{2\beta(1-\beta)q^+(2q^+q^- - \frac{k_\perp^2+m^2}{\beta} - \frac{(k_\perp+q_\perp)^2+m^2}{1-\beta})}$$
$$= \theta(0 \le \beta \le 1)\int d^2k_\perp e^{ik_\perp r_\perp}\frac{f(k,q)}{2(\beta(1-\beta)q^2 - (k_\perp^2 + m^2))}. \quad (27)$$

Straightforward evaluation of the overlap of the two functions (Φ_A, Φ_π) is quite tedious; however we may significantly simplify the evaluations using completeness of the Dirac matrices, viz.

$$\sum_n \Gamma^{(n)}_{\alpha\beta}\Gamma^{(n)}_{\alpha'\beta'} = \delta_{\alpha\alpha'}\delta_{\beta\beta'}, \quad (28)$$

so the product of the numerators of the two DAs is now converted to the effective diagram shown in Fig. 3.

Straightforward evaluation gives

$$F_\mu^{a\to\pi}(q, \Delta) \sim \sum_\Gamma \int d\beta d^2r \Phi_\Gamma^{(\pi)\dagger}(\beta, r_\perp; q - \Delta)\Phi_\Gamma^{(a(\mu))}(\beta, r_\perp; q)$$
$$\sim 4mN_c\int d^2k_\perp \int d\beta \frac{q_\mu(4m^2 + \Delta^2) - \Delta_\mu(4m^2 + 4k\cdot q + q^2) + 2k_\mu(-2k\cdot q + \Delta^2 - q^2 + q\cdot\Delta)}{4(\beta(1-\beta)q^2 - (k_\perp^2 + m^2))(\tilde{\beta}(1-\tilde{\beta})(q-\Delta)^2 - (k_\perp^2 + m^2))}. \quad (29)$$

As we can see, the result is proportional to $\mathcal{O}(m) \sim \mathcal{O}(m_\pi^2)$ and thus is suppressed in the chiral limit. We expect that the same result is valid for the nonperturbative DAs evaluated in the instanton vacuum model.

V. NUMERICAL RESULTS

The Bjorken variable $x = Q^2/(2p\cdot q)$, used at high Q^2, is not appropriate at small Q^2, where it does not have the meaning of a fractional quark momentum any more and may be very small even at low energies. For the case $Q^2 = 0$, where the AR holds, x defined in this way would be zero. Therefore, one should rely on the phenomenological dipole cross section which depends on energy, rather than x. At small Q^2 we employ the s-dependent parametrization of the dipole cross section [69], which is similar to the x-dependent GBW parametrization [7], but is more suitable for soft processes

$$\sigma_{\bar{q}q}(r, s) = \sigma_0(s)(1 - e^{-r^2/R_0^2(s)}), \quad (30)$$

$$R_0(s) = 0.88fm \times \left(\frac{s_0}{s}\right)^{0.14}. \quad (31)$$

These parameters and the scale $s_0 = 1000\ \mathrm{GeV}^2$ are fitted to data on DIS, real photoproduction, and πp scattering.

The function $\sigma_0(s)$ is fixed by the condition

$$\int d^2r\sigma_{\bar{q}q}(r,s)\int_0^1 d\beta|\Psi^\pi(\beta,\vec{r})|^2=\sigma_{\rm tot}^{\pi p}(s). \qquad (32)$$

A. Corrections to the AR

It was pointed out in [32] that the AR (1) applied to the diffractive neutrino production of pions should be broken by absorptive corrections, which affect the left- and right-hand sides of Eq. (1) differently. Therefore, the AR Eq. (1) cannot hold universally, since the magnitude of absorptive corrections is target dependent. The corrections reach maximum in the black-disk limit (e.g. on heavy nuclei), where the AR is severely broken as was demonstrated in Sec. IV. It was revealed in [32] that the AR is not accurate even on a proton target; a deviation of about 30% was estimated for diffractive pion production on a proton. Unfortunately, the baseline for comparison of the left- and right-hand sides of Eq. (1) is ill defined, and it is not clear whether the AR should hold with or without absorptive corrections.

The dipole phenomenology, which is adjusted to data, is free of this uncertainty; it does not need to be corrected for absorption. One can calculate the left- and right-hand sides of Eq. (1) on the same footing. It is important to use the same $\sigma_{\rm tot}^{\pi p}(s)$ in (32), as in the right-hand side of (1). We employ only the Pomeron part of the cross section parametrized as $\sigma_{\rm tot}^{\pi p}(s)=23.6\ {\rm mb}\times(s/s_0)^{0.08}$.

Calculation of the left- and right-hand sides of Eq. (1) clearly demonstrates that absorptive corrections affect them differently. Indeed, the amplitude in the left-hand side of (1) is given by Eqs. (2) and (3). The first term in the dipole cross section (30) is independent of r; therefore its contribution to neutrino-production amplitudes vanishes, as was demonstrated in Sec. IV. So the production amplitude is suppressed by the second exponential term in (30). This suppression becomes stronger with energy, since $R(s)$ decreases, and at very high energies in the Froissart regime the left-hand side of (1) vanishes. At the same time, the pion-proton cross section Eq. (32) is dominated by the first term in (30) and reaches maximum in the Froissart regime.

Now we are in a position to evaluate the accuracy of the AR for diffractive neutrino production of pions on protons. In Fig. 4 we plotted the ratio of the cross sections calculated with the color dipole model [left-hand side of (1)] and using the AR [right-hand side of (1)],

$$K_{\rm AR}(s)=\frac{d\sigma_{\rm dipole}/dtd\nu dQ^2}{d\sigma_{\rm AR}/dtd\nu dQ^2}\bigg|_{Q^2=0,t=0}, \qquad (33)$$

as was defined in [32].

As was expected, $K_{\rm AR}<1$ due to different structures of the absorptive corrections to diffractive pion production and elastic pion scattering cross sections. The deviation of $K_{\rm AR}$ from unity is significant, even somewhat larger than

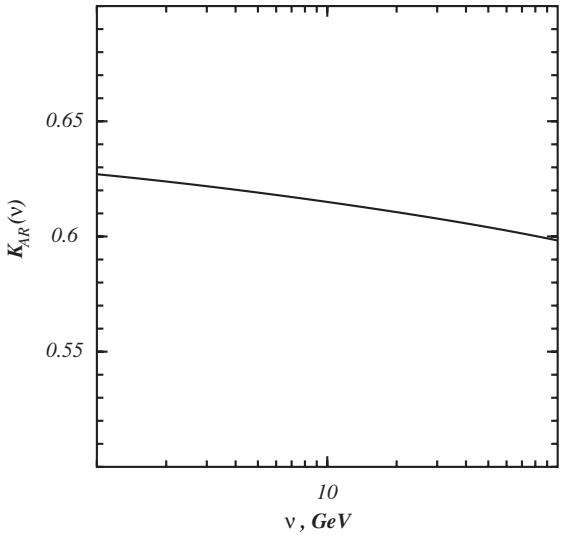

FIG. 4. Ratio of the cross sections calculated within the color dipole model and using the AR (1) at $\Delta_\perp=0$.

was estimated in [32]. The ratio is falling at high energies toward the Froissart limit, where it eventually vanishes when $R_0(s)\to 0$.

B. Predicted cross sections

Most of the data on neutrino production of pions on protons have been available so far only at energies close to the resonance region [28]. Data at higher energies are scarce and have rather low statistics [33,48]. Because the dipole formalism should not be trusted at low energies, we provide predictions for the energy range of the ongoing experiment Minerva at Fermilab [1,26].

The Q^2 dependence of the diffractive cross section deserves special attention. It would be very steep at small Q^2, if the pion dominance were real. However, since the pion pole is terminated due to conservation of the lepton current, the Q^2 dependence is controlled by heavier singularities. In the approximation of an effective singularity at $Q^2=-M^2$ [32] one should expect the dipole form $\propto(Q^2+M^2)^{-2}$. Within the dispersion approach the effective mass scale M is expected to be of the order of 1 GeV [28,29,32]. Within the dipole description the Q^2 dependence is controlled by the IVM mass scale, which is of the order of 700 MeV.

In Fig. 5, we plot the forward diffractive neutrino cross section scaled by the factor $(Q^2+M^2)^2$, where the parameter M is adjusted in a way to provide a flat Q^2 dependence at $Q^2<2\ {\rm GeV}^2$.

Indeed, we found that at $M=0.91$ GeV the scaled cross section is constant up to rather large $Q^2\sim 3\ {\rm GeV}^2$, but substantially deviates from the dipole form at larger Q^2.

The t dependence of the cross section is controlled by the employed model Eq. (5) for impact parameter dependence of the dipole amplitude. The results for t dependence of the invariant cross section are shown in Fig. 6 for several

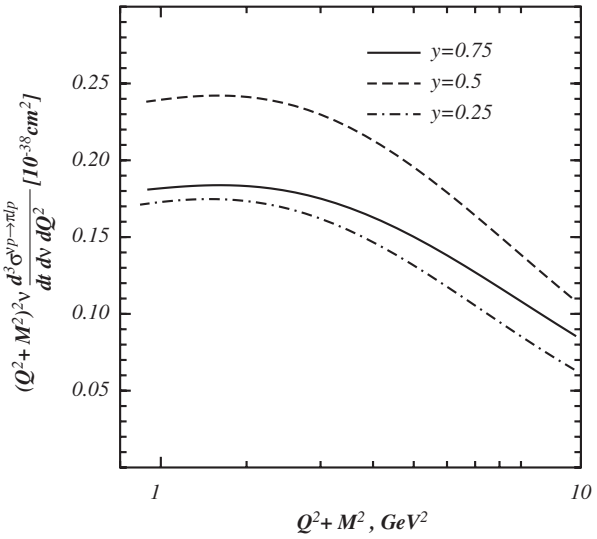

FIG. 5. The Q^2 dependence of the cross section of diffractive neutrino production of pions scaled by factor $(Q^2 + M^2)^2$ at neutrino energy $E_\nu = 20$ GeV and different y. The mass parameter $M = 0.91$ GeV is adjusted to minimize the variations of the scaled cross section at small Q^2.

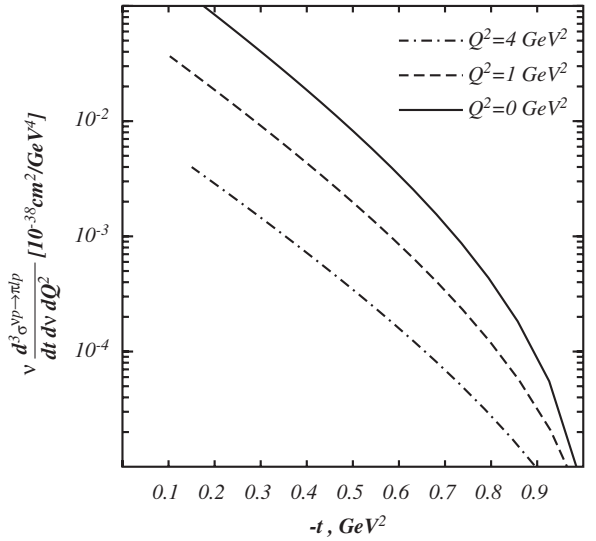

FIG. 6. The t dependence of the cross section of diffractive neutrino production of pions at different Q^2 for neutrino energy $E_\nu = 20$ GeV and $y = 0.5$.

fixed values of E_ν and $Q^2 = 4$ GeV^2. For this calculation we fixed $y = 0.5$.

The forward invariant cross section Eq. (2) of diffractive neutrino production of pions on protons is depicted in Fig. 7 as a function of ν at several fixed values of y and Q^2.

These calculations performed in the dipole approach are controlled in Eq. (3) by the light-cone DAs of the axial current and pion, which we extended to the soft interaction regime based on the instanton vacuum model. It is worth reminding one that neither s-channel resonances, nor

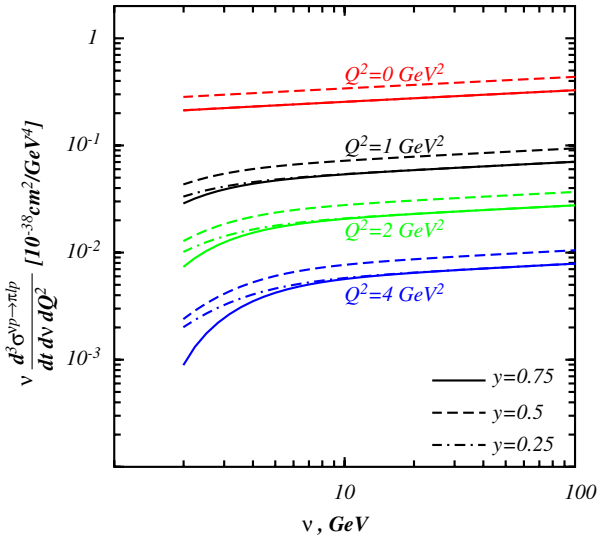

FIG. 7 (color online). Forward neutrino-production cross section of pions as a function of ν at several fixed values of y and Q^2.

Reggeons are included in the parametrization (30) of the universal dipole cross section, so the results can be trusted only at sufficient high-energy ν.

Experimental data for neutrino-production cross section are usually presented as a function of neutrino energy E_ν integrated over ν. Unfortunately, in this form one cannot separate physics of low and high energies. Indeed, the integration over ν results in the finite contribution of the small-ν region, which is dominated by s-channel resonances. This small-ν contribution is constant at any high neutrino energy E_ν and its magnitude is comparable to the diffractive part.

Usually in low statistics experiments one integrates the multidimensional distributions presenting the results as a function of one variable. As such a variable we chose the c.m. energy of the diffraction process, $W = \sqrt{m_N^2 - Q^2 + 2m_N\nu}$. Then we calculate the W distribution as

$$\frac{d\sigma}{dW} = 2W\int d\nu dt dQ^2 \delta(W^2 - (p+q)^2)\frac{d\sigma}{d\nu dt dQ^2}. \tag{34}$$

In the left panel of the Fig. 8 we plotted the W dependence of the cross section (34) for several fixed values of E_ν. We see that the W dependence significantly varies with E_ν; therefore one should average the cross section Eq. (34) weighted with a realistic neutrino energy distribution,

$$\left\langle\frac{d\sigma}{dW}\right\rangle = \int dE_\nu \rho(E_\nu)\frac{d\sigma}{dW}, \tag{35}$$

where the neutrino spectrum $\rho(E_\nu)$ is normalized as

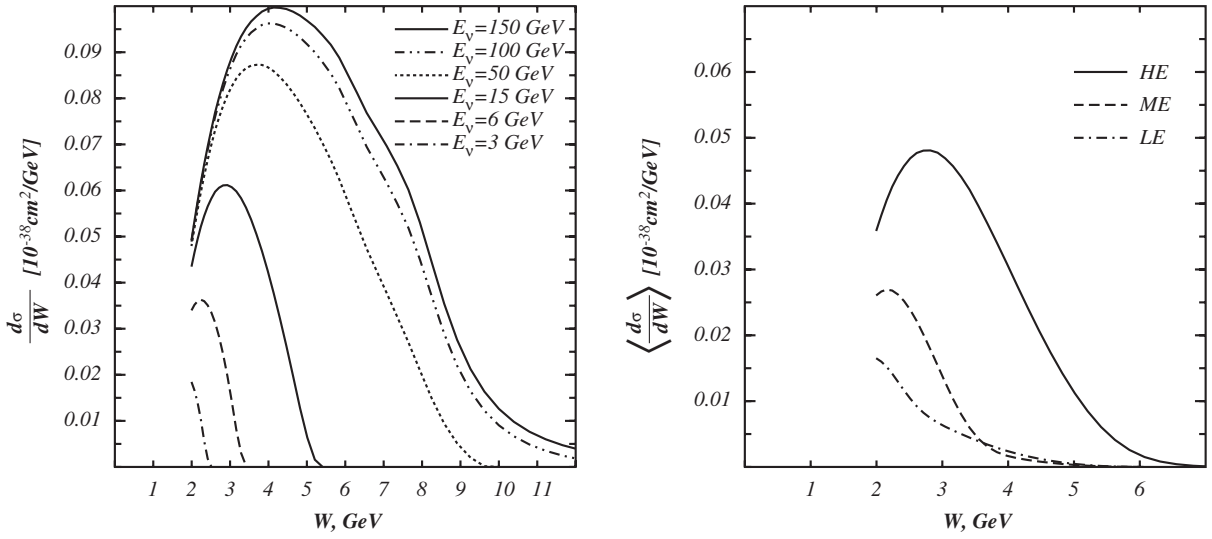

FIG. 8. Left panel: Cross section of diffractive neutrino production $d\sigma/dW$ as a function of W, for fixed neutrino energies E_ν. Right panel: The same cross section $\langle d\sigma/dW \rangle$ weighted with the neutrino spectrum from Minerva [1]; see Eq. (35) for the exact definition.

$$\int dE_\nu \rho(E_\nu) = 1. \tag{36}$$

As an example, we performed calculations with the neutrino energy spectrum of the MINERvA experiment [1]. We considered three different E_ν distributions corresponding to low- (LE), medium- (ME), and high-energy (HE) beam configurations. The results are depicted in the right panel of Fig. 8.

We also compared our results for the W distribution of neutrino diffractive events with data from the WA21 experiment at CERN [48]. We performed averaging over neutrino energy with the spectrum $\rho(E_\nu)$ given in [70]. The results are depicted by a dashed curve in Fig. 9. Since the low-energy region is affected by Reggeons, which we have neglected so far, we added their contribution to the dipole cross section (32),

$$\sigma_{\rm tot}^{\pi p}(s) = [13.6 s^{0.08} + 19.2 s^{-0.45}] \text{ mb}. \tag{37}$$

The result shown by the solid curve describes the data much better. For comparison we also plotted the prediction based on the AR with the realistic pion-proton cross section Eq. (37).

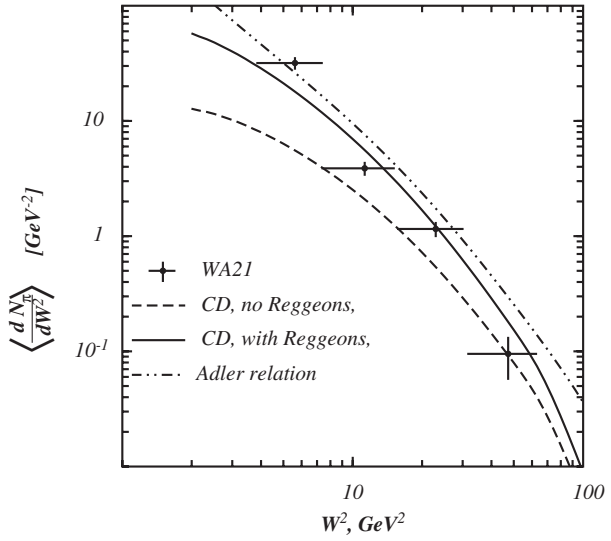

FIG. 9. Comparison of the color dipole prediction with experimental data from [48]. "CD" stands for the color dipole model, either with or without Reggeons. "Adler relation" stands for the evaluation using Adler relation (1) extrapolated to nonzero Q^2 using dipole-type dependence for the Q^2 dependence, $\sim m_A^4/(m_A^2 + Q^2)^2$.

VI. SUMMARY

We developed the dipole description for high-energy neutrino interaction, in particular, at low Q^2, in which the PCAC hypothesis plays an important role. This approach is an alternative to the conventional one based on the dispersion relation for the Q^2 dependent amplitude axial current interaction. While the latter faces the problem of lacking experimental information on most of the diffractive diagonal and off-diagonal amplitudes, the dipole formalism is free of these difficulties. Besides, one can employ the universal dipole cross section [see Eq. (3)], well fixed by numerous data for interactions of the vector current in electromagnetic processes (DIS, photoproduction, etc.).

The important challenge of the dipole description is the construction of the current distribution amplitudes at small Q^2, where the nonperturbative effects are unavoidable. We calculated the distribution amplitudes for the axial current (Sec. III B) and for the pion (Sec. III C) on the same footing, within the instanton vacuum model (Sec. III A). The model possesses the chiral symmetry properties that guarantee a correct behavior controlled by PCAC at small Q^2.

Although the dipole approach does not explicitly involve the intermediate hadronic states, absence of the pion pole can be tested in the "black-disk" regime, where all the partial elastic amplitudes saturate at the unitarity bound. Indeed, the direct calculation performed in Sec. IV confirmed that diffractive pion production ceases and what may happen only if the pion pole does not contribute.

The dipole description also offers an unbiased way to test the AR on a proton target. This relation is expected to be broken by absorptive corrections [32], which are implicitly included in the phenomenological dipole cross section. We rely on the dipole cross section parametrized in the saturation form Eq. (30), well confirmed by data for electromagnetic processes [7]. We found a significant, about 40% deviation from the AR on a proton target (see Fig. 4).

A much stronger breakdown of the AR is expected for nuclei [32], and we plan to evaluate those effects employing the techniques developed here.

ACKNOWLEDGMENTS

We are grateful to Genya Levin for numerous discussions and improving comments, and to Sasha Dorokhov for the fruitful discussion of the pion distribution amplitudes. We thank Jorge Morfin for the interest in our results and advice regarding comparison with data. This work was supported in part by Fondecyt (Chile) Grants No. 1090073, No. 1090291, and No. 1100287, and by Conicyt-DFG Grant No. 084-2009.

APPENDIX: DISTRIBUTION AMPLITUDES IN THE INSTANTON VACUUM MODEL

In this Appendix we present the results of calculation of the DAs for the axial current and pion performed in the IVM.

1. Axial DAs

There are eight independent axial DAs defined in (15)–(18),

$$\langle 0|\bar\psi(y)\gamma_\mu\gamma_5\psi(x)|A(q)\rangle = if_A^2\int_0^1 du e^{i(up\cdot y+\bar up\cdot x)}\Big[p_\mu\frac{e^{(\lambda)}\cdot z}{p\cdot z}\Phi_\parallel(u) + e_\mu^{(\lambda=\perp)}g_\perp^{(a)}(u) - \frac{1}{2}z_\mu\frac{e^{(\lambda)}\cdot z}{(p\cdot z)^2}f_A^2 g_3(u)\Big], \quad \text{(A1)}$$

$$\langle 0|\bar\psi(y)\gamma_\mu\psi(x)|A(q)\rangle = -if_A^2\epsilon_{\mu\nu\rho\sigma}e_\nu^{(\lambda)}p_\rho z_\sigma\int_0^1 du e^{i(up\cdot y+\bar up\cdot x)}\frac{g_\perp^{(v)}(u)}{4}, \quad \text{(A2)}$$

$$\langle 0|\bar\psi(y)\sigma_{\mu\nu}\gamma_5\psi(x)|A(q)\rangle = f_A\int_0^1 du e^{i(up\cdot y+\bar up\cdot x)}\Big[(e_\mu^{(\lambda=\perp)}p_\nu - e_\nu^{(\lambda=\perp)}p_\mu)\Phi_\perp(u) + \frac{e^{(\lambda)}\cdot z}{(p\cdot z)^2}f_A^2(p_\mu z_\nu - p_\nu z_\mu)h_\parallel^{(t)}(u) + \frac{1}{2}(e_\mu^{(\lambda)}z_\nu - e_\nu^{(\lambda)}z_\mu)\frac{f_A^2}{p\cdot z}h_3(u)\Big], \quad \text{(A3)}$$

$$\langle 0|\bar\psi(y)\gamma_5\psi(x)|A(q)\rangle = f_A^3 e^{(\lambda)}\cdot z\int_0^1 du e^{i(up\cdot y+\bar up\cdot x)}\frac{h_\parallel^{(p)}(u)}{2}. \quad \text{(A4)}$$

After tedious but straightforward calculations we arrive at

$$\Phi_\parallel(u,\vec r_\perp) = \frac{1}{if_A^2 n\cdot e^{(\lambda)}}\int\frac{dz}{2\pi}e^{i(u-1/2)z}\left\langle 0\left|\bar\psi\left(-\frac{z}{2}n-\frac{\vec r_\perp}{2}\right)\hat n\gamma_5\psi\left(\frac{z}{2}n+\frac{\vec r_\perp}{2}\right)\right|A^{(\lambda)}(q)\right\rangle = \quad \text{(A5)}$$

$$= \frac{8N_c}{if_A^2}\int\frac{dl^-d^2l_\perp}{(2\pi)^4}e^{-i\vec l_\perp\cdot\vec r_\perp} \quad \text{(A6)}$$

$$\left[\frac{\mu(l)\mu(l+q)+l_\perp^2+(\frac{1}{4}-u^2)q^2}{(l^2+\mu^2(l))((l+q)^2+\mu^2(l+q))} + \frac{M(f(l+q)-f(l))^2(2l^- - q^2(u-\frac{1}{2}))(\mu(l)(u+\frac{1}{2})-\mu(l+q)(u-\frac{1}{2}))}{((l+q)^2-l^2)(l^2+\mu^2(l))((l+q)^2+\mu^2(l+q))}\right]_{l^+=(u-1/2)q^+}, \quad \text{(A7)}$$

$$\Phi_\perp(u,\vec r_\perp) = \frac{1}{2f_A}\int\frac{dz}{2\pi}e^{i(u-1/2)z}\left\langle 0\left|\bar\psi\left(-\frac{z}{2}n\right)\sigma_{\nu\rho}\gamma_5(e_\nu^{(\lambda=\perp)}n_\rho - e_\rho^{(\lambda=\perp)}n_\nu)\psi\left(\frac{z}{2}n\right)\right|A^{(\lambda=\perp)}(q)\right\rangle$$
$$= \frac{4N_c}{\pi f_A}\int\frac{dl^-d^2l_\perp}{(2\pi)^4}e^{-i\vec l_\perp\cdot\vec r_\perp}\left[\frac{(u-\frac{1}{2})\mu(l+q)+(u+\frac{1}{2})\mu(l)}{(l^2+\mu^2(l))((l+q)^2+\mu^2(l+q))} - \frac{l_{\mu_\perp}^2}{(l+q)^2-l^2}\frac{M(f(l+q)-f(l))^2}{(l^2+\mu^2(l))((l+q)^2+\mu^2(l+q))}\right]_{l^+=(u-1/2)q^+},$$

$$g_\perp^{(a)}(u,\vec{r}_\perp) = \frac{1}{if_A^2}\int\frac{dz}{2\pi}e^{i(u-1/2)z}\left\langle 0\left|\bar\psi\left(-\frac{z}{2}n\right)\hat e^{(\lambda=\perp)}\gamma_5\psi\left(\frac{z}{2}n\right)\right|A^{(\lambda=\perp)}(q)\right\rangle$$
$$= \frac{4N_c}{i\pi f_A^2}\int\frac{dl^-d^2l_\perp}{(2\pi)^4}e^{-i\vec{l}_\perp\cdot\vec{r}_\perp}\left[\frac{(\mu(l)\mu(l+q)-l^2-l\cdot q)+l_\perp^2}{(l^2+\mu^2(l))((l+q)^2+\mu^2(l+q))}\right.$$
$$\left.-\frac{l_{\mu\perp}^2}{(l+q)^2-l^2}\frac{M(f(l+q)-f(l))^2(\mu(l+q)-\mu(l))}{(l^2+\mu^2(l))((l+q)^2+\mu^2(l+q))}\right]_{l^+=(u-1/2)q^+},$$

$$g_\perp^{(v)}(u,\vec{r}_\perp) = \frac{4i}{f_A^2}\text{coefficient}\left(\int\frac{dz}{2\pi}e^{i(u-1/2)z}\left\langle 0\left|\bar\psi\left(-\frac{z}{2}n\right)\hat e^{(\lambda=\perp)}\gamma_\mu\psi\left(\frac{z}{2}n\right)\right|A^{(\lambda=\perp)}(q)\right\rangle,\epsilon_{\mu\nu\rho\sigma}e_\nu^{(\lambda)}p_\rho n_\sigma\right)$$
$$= \frac{32N_c}{f_A^2}\int\frac{dl^+}{2\pi}\frac{1}{q^+}\delta\left(\frac{l^+}{q^+}-u+\frac{1}{2}\right)\int\frac{dl^-d^2l_\perp}{(2\pi)^4}e^{-i\vec{l}_\perp\cdot\vec{r}_\perp}\left[\frac{q\cdot l-q^2(u-\frac{1}{2})}{(l^2+\mu^2(l))((l+q)^2+\mu^2(l+q))}\right]_{l^+=(u-1/2)q^+},$$

$$h_\parallel^{(t)}(u,\vec{r}_\perp) = -\frac{1}{2f_A^3e^{(\lambda)}\cdot n}\int\frac{dz}{2\pi}e^{i(u-1/2)z}\left\langle 0\left|\bar\psi\left(-\frac{z}{2}n\right)\sigma_{\nu\rho}\gamma_5(p_\nu n_\rho-p_\rho n_\nu)\psi\left(\frac{z}{2}n\right)\right|A^{(\lambda)}(q)\right\rangle$$
$$= \frac{8N_c}{f_A^3}\int\frac{dl^-d^2l_\perp}{(2\pi)^4}e^{-i\vec{l}_\perp\cdot\vec{r}_\perp}\left[\frac{\mu(l+q)(l^-+(u-\frac{1}{2})\frac{q^2}{2})+\mu(l)(l^-+(u+\frac{3}{2})\frac{q^2}{2})}{(l^2+\mu^2(l))((l+q)^2+\mu^2(l+q))}\right.$$
$$\left.+\frac{2((l^-)^2-(u-\frac{1}{2})^2\frac{q^4}{4})M(f(l+q)-f(l))^2}{((l+q)^2-l^2)(l^2+\mu^2(l))((l+q)^2+\mu^2(l+q))}\right]_{l^+=(u-1/2)q^+},$$

$$h_\parallel^{(p)}(u,\vec{r}_\perp) = \frac{1}{(f_A^3e^{(\lambda)}\cdot n)}\int\frac{dz}{2\pi}e^{i(u-1/2)z}\left\langle 0\left|\bar\psi\left(-\frac{z}{2}n\right)\hat e^{(\lambda=\perp)}\gamma_5\psi\left(\frac{z}{2}n\right)\right|A^{(\lambda=\perp)}(q)\right\rangle$$
$$= -\frac{8N_c}{f_A^3}\int\frac{dl^+}{2\pi}\frac{1}{q^+}\delta\left(\frac{l^+}{q^+}-u+\frac{1}{2}\right)\int\frac{dl^-d^2l_\perp}{(2\pi)^4}e^{-i\vec{l}_\perp\cdot\vec{r}_\perp}\left[\frac{(\mu(l)-\mu(l+q))(l^-+(\frac{1}{2}-u)\frac{q^2}{2})}{(l^2+\mu^2(l))((l+q)^2+\mu^2(l+q))}\right.$$
$$\left.-\frac{(-l_\perp^2+2ul^-+(u-\frac{1}{2})\frac{q^2}{2}+\mu(l)\mu(l+q))}{(l+q)^2-l^2}\frac{M(f(l+q)-f(l))^2(2l^--q^2(u-\frac{1}{2}))}{(l^2+\mu^2(l))((l+q)^2+\mu^2(l+q))}\right]_{l^+=(u-1/2)q^+},$$

$$g_3(u,\vec{r}_\perp) = -\frac{2}{f_A^2e^{(\lambda)}\cdot n}\int\frac{dz}{2\pi}e^{i(u-1/2)z}\left\langle 0\left|\bar\psi\left(-\frac{z}{2}n\right)\hat p\gamma_5\psi\left(\frac{z}{2}n\right)\right|A^{(\lambda)}(q)\right\rangle$$
$$= -\frac{8N_c}{f_A^2}\int\frac{dl^-d^2l_\perp}{(2\pi)^4}e^{-i\vec{l}_\perp\cdot\vec{r}_\perp}\left[\frac{2(l^-)^2+l^-q^2-(\mu(l)\mu(l+q)+l_\perp^2)\frac{q^2}{2}}{(l^2+\mu^2(l))((l+q)^2+\mu^2(l+q))}\right.$$
$$\left.-\frac{(\mu(l)(l^-+\frac{q^2}{2})-\mu(l+q)l^-)}{((l+q)^2-l^2)}\frac{M(f(l+q)-f(l))^2(l^--\frac{q^2}{2}(u-\frac{1}{2}))}{(l^2+\mu^2(l))((l+q)^2+\mu^2(l+q))}\right]_{l^+=(u-1/2)q^+},$$

$$h_3(u,\vec{r}_\perp) = \frac{1}{f_A^3}\int\frac{dz}{2\pi}e^{i(u-1/2)z}\left\langle 0\left|\bar\psi\left(-\frac{z}{2}n\right)\sigma_{\nu\rho}\gamma_5(e_\nu^{(\lambda=\perp)}p_\rho-e_\rho^{(\lambda=\perp)}p_\nu)\psi\left(\frac{z}{2}n\right)\right|A^{(\lambda=\perp)}(q)\right\rangle$$
$$= \frac{16N_c}{f_A^3}\int\frac{dl^-d^2l_\perp}{(2\pi)^4}e^{-i\vec{l}_\perp\cdot\vec{r}_\perp}\left[\frac{l_-\mu(l+q)+(l_-+q_-)\mu(l)}{(l^2+\mu^2(l))((l+q)^2+\mu^2(l+q))}-l_{\mu\perp}^2\frac{M(f(l+q)-f(l))^2}{(l^2+\mu^2(l))((l+q)^2+\mu^2(l+q))}\right]_{l^+=(u-1/2)q^+}.$$

2. Pion DAs

For the pion there are four independent pion DAs defined in (21)–(23),

$$\langle 0|\bar\psi(y)\gamma_\mu\gamma_5\psi(x)|\pi(q)\rangle = if_\pi\int_0^1 du e^{i(up\cdot y+\bar up\cdot x)}\Big(p_\mu\phi_{2;\pi}(u)+\frac{1}{2}\frac{z_\mu}{(p\cdot z)}\psi_{4;\pi}(u)\Big), \tag{A8}$$

$$\langle 0|\bar\psi(y)\gamma_5\psi(x)|\pi(q)\rangle = -if_\pi\frac{m_\pi^2}{m_u+m_d}\int_0^1 du e^{i(up\cdot y+\bar up\cdot x)}\phi_{3;\pi}^{(p)}(u), \tag{A9}$$

$$\langle 0|\bar\psi(y)\sigma_{\mu\nu}\gamma_5\psi(x)|\pi(q)\rangle = -\frac{i}{3}f_\pi\frac{m_\pi^2}{m_u+m_d}\int_0^1 du\phi_{3;\pi}^{(\sigma)}(u)\frac{e^{i(up\cdot y+\bar up\cdot x)}}{p\cdot z}(p_\mu z_\nu - p_\nu z_\mu). \tag{A10}$$

Eventually we arrive at the following structures in the pion DA:

$$\begin{aligned}\phi_{2;\pi}(u,\vec r_\perp) &= \frac{1}{if_\pi}\int\frac{dz}{2\pi}e^{i(u-1/2)z}\Big\langle 0\Big|\bar\psi\Big(-\frac{z}{2}n-\frac{\vec r_\perp}{2}\Big)\hat n\gamma_5\psi\Big(\frac{z}{2}n+\frac{\vec r_\perp}{2}\Big)\Big|\pi(q)\Big\rangle\\ &= \frac{8N_c}{f_\pi}\int\frac{dl^-d^2l_\perp}{(2\pi)^4}e^{-i\vec l_\perp\cdot\vec r_\perp}\Big[Mf(l)f(l+q)\frac{\mu(l)(u+\frac12)-\mu(l+q)(u-\frac12)}{(l^2+\mu^2(l))((l+q)^2+\mu^2(l+q))}\Big]_{l^+=(u-1/2)q^+},\end{aligned} \tag{A11}$$

$$\begin{aligned}\psi_{4;\pi}(u,\vec r_\perp) &= \frac{2}{if_\pi}\int\frac{dz}{2\pi}e^{i(u-1/2)z}\Big\langle 0\Big|\bar\psi\Big(-\frac{z}{2}n-\frac{\vec r_\perp}{2}\Big)\hat p\gamma_5\psi\Big(\frac{z}{2}n+\frac{\vec r_\perp}{2}\Big)\Big|\pi(q)\Big\rangle\\ &= \frac{16N_c}{f_\pi}\int\frac{dl^-d^2l_\perp}{(2\pi)^4}e^{-i\vec l_\perp\cdot\vec r_\perp}\Big[Mf(l)f(l+q)\frac{\mu(l)(l_-+q_-)-\mu(l+q)l_-}{(l^2+\mu^2(l))((l+q)^2+\mu^2(l+q))}\Big]_{l^+=(u-1/2)q^+},\end{aligned} \tag{A12}$$

$$\begin{aligned}\phi_{3;\pi}^{(p)}(u,\vec r_\perp) &= \frac{1}{f_\pi}\frac{m_u+m_d}{m_\pi^2}\int\frac{dz}{2\pi}e^{i(u-1/2)z}\Big\langle 0\Big|\bar\psi\Big(-\frac{z}{2}n-\frac{\vec r_\perp}{2}\Big)\gamma_5\psi\Big(\frac{z}{2}n+\frac{\vec r_\perp}{2}\Big)\Big|\pi(q)\Big\rangle\\ &= \frac{8N_c}{f_\pi}\frac{m_u+m_d}{m_\pi^2}\int\frac{dl^-d^2l_\perp}{(2\pi)^4}e^{-i\vec l_\perp\cdot\vec r_\perp}\Big[Mf(l)f(l+q)\frac{\mu(l)\mu(l+q)+l^2+l\cdot q}{(l^2+\mu^2(l))((l+q)^2+\mu^2(l+q))}\Big]_{l^+=(u-1/2)q^+},\end{aligned} \tag{A13}$$

$$\begin{aligned}\phi_{3;\pi}^{(\sigma)}(u,\vec r_\perp) &= \frac{3i}{2f_\pi}\frac{m_u+m_d}{m_\pi^2}\int\frac{dz}{2\pi}e^{i(u-1/2)z}\Big\langle 0\Big|\bar\psi\Big(-\frac{z}{2}n-\frac{\vec r_\perp}{2}\Big)(p_\mu n_\nu-p_\nu n_\mu)\sigma_{\mu\nu}\gamma_5\psi\Big(\frac{z}{2}n+\frac{\vec r_\perp}{2}\Big)\Big|\pi(q)\Big\rangle\\ &= -\frac{24N_c}{f_\pi}\frac{m_u+m_d}{m_\pi^2}\int\frac{dl^-d^2l_\perp}{(2\pi)^4}e^{-i\vec l_\perp\cdot\vec r_\perp}\Big[Mf(l)f(l+q)\frac{q_+l_- - \frac{q^2}{2}(u-\frac12)}{(l^2+\mu^2(l))((l+q)^2+\mu^2(l+q))}\Big]_{l^+=(u-1/2)q^+}.\end{aligned} \tag{A14}$$

The details of calculation of the distribution amplitudes will be presented elsewhere.

3. Vector current DAs

The vector current DAs were derived in [60],

$$\langle 0|\bar\psi(y)\gamma_\mu\gamma_5\psi(x)|V(q)\rangle = e_q f_{3\gamma}f_\gamma^a(q)\epsilon_{\mu\nu\rho\sigma}e_\nu^{(\lambda)}p_\rho z_\sigma\int_0^1 du e^{i(up\cdot y+\bar up\cdot x)}\psi_\gamma^{(a)}(u,q^2), \tag{A15}$$

$$\begin{aligned}\langle 0|\bar\psi(y)\gamma_\mu\psi(x)|V(q)\rangle = e_q f_{3\gamma}f_{\perp\gamma}^v(q)\int_0^1 du e^{i(up\cdot y+\bar up\cdot x)}\Big[&p_\mu(e^{(\lambda)}\cdot n)\frac{f_{\parallel\gamma}^{(v)}(q)}{f_{\perp\gamma}^{(v)}(q)}\phi_\parallel(u,q^2)+e_\mu^{(\lambda=\perp)}\psi_{\perp\gamma}^{(v)}(u,q^2)\\ &+n_\mu(e^{(\lambda)}\cdot n)h_\gamma^{(v)}(u,q^2)\Big],\end{aligned} \tag{A16}$$

$$\langle 0|\bar{\psi}(y)\sigma_{\mu\nu}\psi(x)|V(q)\rangle = ie_q\langle\bar{q}q\rangle f_{\perp\gamma}^t(q^2)\int_0^1 du e^{i(up\cdot y+\bar{u}p\cdot x)}[(e_\mu^{(\lambda=\perp)}p_\nu - e_\nu^{(\lambda=\perp)}p_\mu)\chi_m\phi_{\perp\gamma}(u,q^2) + (e^{(\lambda)}\cdot n)(p_\mu n_\nu - p_\nu n_\mu)\psi_\gamma^{(t)}(u,q^2) + (e_\mu^{(\lambda=\perp)}n_\nu - e_\nu^{(\lambda=\perp)}n_\mu)h_\gamma^{(t)}(u,q^2)], \quad \text{(A17)}$$

$$\langle 0|\bar{\psi}(y)\psi(x)|V(q)\rangle = f_A^\perp m_A^2 e^{(\lambda)}\cdot z\int_0^1 du e^{i(up\cdot y+\bar{u}p\cdot x)}\mathcal{D}_T(u,q^2), \quad \text{(A18)}$$

where the distribution amplitudes $\phi_\parallel$, $\phi_{\perp\gamma}$ have twist-2, $\psi_{\perp\gamma}^{(v)}$, $\psi_\gamma^{(a)}$, and $\psi_\gamma^{(t)}$; $\mathcal{D}_T$ have twist-3; and $h_\gamma^{(v)}$, $h_\gamma^{(t)}$ have twist-4. The form factors $f_\gamma^a(q)$, $f_{\perp\gamma}^v(q)$, and $f_{\perp\gamma}^t(q^2)$ and normalization constants $f_{3\gamma}$, χ_m, and $f_A^\perp$ are discussed in detail in [60].

[1] D. Drakoulakos *et al.* (Minerva Collaboration), arXiv:hep-ex/0405002.
[2] H. Fraas, B. J. Read, and D. Schildknecht, Nucl. Phys. **B86**, 346 (1975).
[3] P. Ditsas, B. J. Read, and G. Shaw, Nucl. Phys. **B99**, 85 (1975).
[4] G. Shaw, Phys. Rev. D **47**, R3676 (1993).
[5] K. Goeke, V. Guzey, and M. Siddikov, Eur. Phys. J. A **36**, 49 (2008).
[6] B. Z. Kopeliovich, L. I. Lapidus, and A. B. Zamolodchikov, Pis'ma Zh. Eksp. Teor. Fiz. **33**, 612 (1981) [http://www.jetpletters.ac.ru/ps/454/article_7188.shtml] (in Russian) [JETP Lett. **33**, 595 (1981)] [http://www.jetpletters.ac.ru/ps/1511/article_23095.shtml].
[7] K. J. Golec-Biernat and M. Wüsthoff, Phys. Rev. D **59**, 014017 (1998).
[8] K. J. Golec-Biernat, Acta Phys. Pol. B **35**, 3103 (2004) [http://th-www.if.uj.edu.pl/acta/vol35/abs/v35p3103.htm].
[9] J. Hufner, Yu. P. Ivanov, B. Z. Kopeliovich, and A. V. Tarasov, Phys. Rev. D **62**, 094022 (2000).
[10] B. Z. Kopeliovich, I. Schmidt, and M. Siddikov, Phys. Rev. D **79**, 034019 (2009).
[11] B. Z. Kopeliovich, I. Schmidt, and M. Siddikov, Phys. Rev. D **80**, 054005 (2009).
[12] B. Z. Kopeliovich, I. Schmidt, and M. Siddikov, Phys. Rev. D **81**, 094013 (2010).
[13] B. Z. Kopeliovich, I. Schmidt, and M. Siddikov, Phys. Rev. D **82**, 014017 (2010).
[14] R. Fiore and V. R. Zoller, Phys. Lett. B **632**, 87 (2006).
[15] R. Fiore and V. R. Zoller, Pis'ma Zh. Eksp. Teor. Fiz. **82**, 435 (2005) [http://www.jetpletters.ac.ru/ps/1047/article_15937.shtml] [JETP Lett. **82**, 385 (2005)].
[16] R. Fiore and V. R. Zoller, JETP Lett. **87**, 524 (2008).
[17] R. Fiore and V. R. Zoller, Phys. Lett. B **681**, 32 (2009).
[18] B. Floter, B. Z. Kopeliovich, H. J. Pirner, and J. Raufeisen, Phys. Rev. D **76**, 014009 (2007).
[19] M. B. Gay Ducati, M. M. Machado, and M. V. T. Machado, Phys. Rev. D **79**, 073008 (2009).
[20] M. B. Gay Ducati, M. M. Machado, and M. V. T. Machado, Braz. J. Phys. **38**, 487 (2008).
[21] M. B. G. Ducati, M. M. Machado, and M. V. T. Machado, Phys. Lett. B **644**, 340 (2007).
[22] M. V. T. Machado, Phys. Rev. D **75**, 093008 (2007).
[23] M. V. T. Machado, Eur. Phys. J. C **59**, 769 (2009).
[24] M. V. T. Machado, Phys. Rev. D **78**, 034016 (2008).
[25] M. V. T. Machado, arXiv:0905.4516.
[26] K. S. McFarland (MINERvA Collaboration), Nucl. Phys. B, Proc. Suppl. **159**, 107 (2006).
[27] C. A. Piketty and L. Stodolsky, Nucl. Phys. **B15**, 571 (1970).
[28] B. Z. Kopeliovich and P. Marage, Int. J. Mod. Phys. A **8**, 1513 (1993).
[29] A. A. Belkov and B. Z. Kopeliovich, Yad. Fiz. **46**, 874 (1987) [Sov. J. Nucl. Phys. **46**, 499 (1987)].
[30] S. L. Adler, Phys. Rev. **135**, B963 (1964).
[31] S. L. Adler and Y. Dothan, Phys. Rev. **151**, 1267 (1966).
[32] B. Z. Kopeliovich, I. K. Potashnikova, I. Schmidt, and M. Siddikov, arXiv:1105.1711 [Phys. Rev. C (to be published)].
[33] J. Bell *et al.*, Phys. Rev. Lett. **41**, 1008 (1978).
[34] J. D. Bjorken and J. Kogut, Phys. Rev. D **8**, 1341 (1973).
[35] B. Z. Kopeliovich, L. I. Lapidus, S. V. Mukhin, and A. B. Zamolodchikov, Sov. Phys. JETP **77**, 451 (1979).
[36] M. H. Ahn *et al.* (K2K Collaboration), Phys. Rev. Lett. **90**, 041801 (2003).
[37] M. Hasegawa *et al.* (K2K Collaboration), Phys. Rev. Lett. **95**, 252301 (2005).
[38] R. Gran *et al.* (K2K Collaboration), Phys. Rev. D **74**, 052002 (2006).
[39] A. A. Aguilar-Arevalo *et al.* (MiniBooNE Collaboration), Phys. Rev. Lett. **100**, 032301 (2008).
[40] A. A. Aguilar-Arevalo *et al.* (MiniBooNE Collaboration), Phys. Lett. B **664**, 41 (2008).
[41] G. P. Zeller *et al.* (NuTeV Collaboration), Phys. Rev. Lett. **88**, 091802 (2002); **90**, 239902 (2003).
[42] M. Goncharov *et al.* (NuTeV Collaboration), Phys. Rev. D **64**, 112006 (2001).
[43] A. Romosan *et al.* (CCFR/NuTeV Collaboration), Phys. Rev. Lett. **78**, 2912 (1997).
[44] C. Amsler *et al.* (Particle Data Group), Phys. Lett. B **667**, 1 (2008).
[45] B. Z. Kopeliovich, Zh. Eksp. Teor. Fiz. **97**, 1418 (1990) [Sov. Phys. JETP **70**, 801 (1990)] [http://www.jetp.ac.ru/cgi-bin/index/r/97/5/p1418?a=list].
[46] B. Z. Kopeliovich, Phys. Lett. B **227**, 461 (1989).
[47] B. Z. Kopeliovich, Nucl. Phys. B, Proc. Suppl. **139**, 219 (2005).

[48] P. Allen *et al.* (Aachen-Birmingham-Bonn-CERN-London-Munich-Oxford Collaboration), Nucl. Phys. **B264**, 221 (1986).
[49] Y. Ashie *et al.* (Super-Kamiokande Collaboration), Phys. Rev. D **71**, 112005 (2005).
[50] Q. R. Ahmad *et al.* (SNO Collaboration), Phys. Rev. Lett. **89**, 011301 (2002).
[51] M. H. Ahn *et al.* (K2K Collaboration), Phys. Rev. D **74**, 072003 (2006).
[52] K. Eguchi *et al.* (KamLAND Collaboration), Phys. Rev. Lett. **90**, 021802 (2003).
[53] B. Z. Kopeliovich, H. J. Pirner, A. H. Rezaeian, and I. Schmidt, Phys. Rev. D **77**, 034011 (2008).
[54] B. Z. Kopeliovich, A. H. Rezaeian, and I. Schmidt, Phys. Rev. D **78**, 114009 (2008).
[55] B. Z. Kopeliovich, I. K. Potashnikova, I. Schmidt, and J. Soffer, Phys. Rev. D **78**, 014031 (2008).
[56] J. B. Bronzan, G. L. Kane, and U. P. Sukhatme, Phys. Lett. **49B**, 272 (1974).
[57] T. Schafer and E. V. Shuryak, Rev. Mod. Phys. **70**, 323 (1998).
[58] D. Diakonov and V. Y. Petrov, Nucl. Phys. **B272**, 457 (1986).
[59] D. Diakonov, M. V. Polyakov, and C. Weiss, Nucl. Phys. **B461**, 539 (1996).
[60] A. E. Dorokhov, W. Broniowski, and E. R. Arriola, Phys. Rev. D **74**, 054023 (2006).
[61] I. V. Anikin, A. E. Dorokhov, and L. Tomio, Fiz. Elem. Chastits At. Yadra **31**, 1023 (2000) [Phys. Part. Nucl. **31**, 509 (2000)].
[62] A. E. Dorokhov and W. Broniowski, Eur. Phys. J. C **32**, 79 (2003).
[63] K. Goeke, M. M. Musakhanov, and M. Siddikov, Phys. Rev. D **76**, 076007 (2007).
[64] K. C. Yang, Nucl. Phys. **B776**, 187 (2007).
[65] P. Ball, V. M. Braun, and A. Lenz, J. High Energy Phys. 05 (2006) 004.
[66] V. Y. Petrov, M. V. Polyakov, R. Ruskov, C. Weiss, and K. Goeke, Phys. Rev. D **59**, 114018 (1999).
[67] A. E. Dorokhov, Czech. J. Phys. **56**, F169 (2006) [Braz. J. Phys. **37**, 819 (2007)].
[68] A. E. Dorokhov, Pis'ma Zh. Eksp. Teor. Fiz. **77**, 68 (2003) [http://www.jetpletters.ac.ru/ps/15/article_168.shtml] [JETP Lett. **77**, 63 (2003)].
[69] B. Z. Kopeliovich, A. Schäfer, and A. V. Tarasov, Phys. Rev. D **62**, 054022 (2000).
[70] G. T. Jones *et al.* (Birmingham-CERN-London-Munich-Oxford-London Collaboration and WA21 Collaboration), Z. Phys. C **37**, 25 (1987).